CI&CEQ
Chemical Industry & Chemical Engineering Quarterly

Available on line at
Association of the Chemical Engineers of Serbia AChE
www.ache.org.rs/CICEQ

Chem. Ind. Chem. Eng. Q. 28 (1) 19–28 (2022) CI&CEQ

GUNAY BAYDAR-ATAK[1]
MERT AKIN INSEL[1]
MUHAMMED ENES ORUC[2]
HASAN SADIKOGLU[1]

[1]Yildiz Technical University, Department of Chemical Engineering, Esenler, İstanbul, Turkey
[2]Gebze Technical University, Department of Chemical Engineering, Gebze, Kocaeli, Turkey

SCIENTIFIC PAPER

UDC 66.017:616.155.2:519.8:544

OPTIMIZATION OF MEGAKARYOCYTE TRAPPING FOR PLATELET FORMATION IN MICROCHANNELS

Article Highlights

- A microfluidic chip has been designed and simulated to maximize MKs trapping
- The flow rate ratios and the effect of angle between the inlets have been investigated
- The flow rate ratio is more significant than the angle between the inlets on the trapping of MKs
- Based on the results, the ultimate MKs trapping is achieved when the angle is 50.46°

Abstract

Platelets (PLTs) are responsible for stopping bleeding. They are small cell fragments produced from megakaryocytes (MKs) in the bone marrow. Low platelet count is a significant health problem for a patient. PLTs can usually be stored for up to 5 days prior to transfusion. Instantaneous production of PLTs from isolated and stored MKs is crucial for the patient's health. Thanks to microfluidic platforms, PLTs can be produced instantaneously from MKs. Herein, we have computationally studied fluid dynamics in the microchannels with slit structures and different inlet geometries. Analysis of the flow dynamics was performed by the commercial analysis software. The effects of flow rates and the angle between the inlet channels on the MKs trapping were investigated. The optimization of the angle between inlet channels and flow rates of main and pressure flows was done with response surface methodology (RSM) by counting the trapped MKs. The optimum conditions lead to the percentage of trapped MKs being 100 with a relative deviation of <1%. We also concluded that flow rates to trapping a higher amount of MKs are as important as the angle between the inlet channels.

Keywords: microfluidics, biotechnology, mathematical modeling, platelet, COMSOL Multiphysics.

Platelets (PLTs) are a component of blood and vital for hemostasis and thrombosis. They play an essential role in wound repair, inflammatory reactions, angiogenesis, lymph vessel separation, and tumor metastasis. These small and essential cells are derived from the megakaryocytes (MKs) [1,2], and approximately 1×10^{11} PLTs are formed per day in a human body [3]. Once PLTs are required in larger quantities, units are derived entirely from human donors [4-6]. In the United States, more than 2.17 million apheresis equivalent PLT units are transfused per year, more than a cost of 10^9 per year [7,8]. Although the demand for PLT transfusion has increased significantly in the last decade, a significant PLT shortage is a challenge due to the presence of a static donor pool and about 5-day PLT shelf life correlated with bacterial contamination and PLT degradation storage [9]. Besides, artificial PLTs produced in biotechnological processes have not taken over from the physiological PLT products. It is, however, indispensable to produce artificial PLTs by instant, high-throughput, and rapid methods [1].

The MKs are broken down into PLTs during transit to capillaries under high shear stress in bone marrow [1]. The proposed mechanism starts with the erosion of an MK. With the erosion, ramified large pseudopodial-like structures are produced to obtain

Correspondence: H. Sadikoglu, Yildiz Technical University, Faculty of Chemical and Metallurgical, Department of Chemical Engineering, 34210, Esenler, Istanbul, Turkey.
E-mail: hsadik@yildiz.edu.tr
Paper received:24 December, 2020
Paper revised: 31 March, 2021
Paper accepted: 7 May, 2021

https://doi.org/10.2298/CICEQ201224012B

uniform diameter (2-4 μm) tubular projections. ProPLT elongations extend outwardly at a steady rate of ~1 μm/min and generally reach lengths of 0.5-1 mm [10]. After infiltrating into the bloodstream, the proPLTs are converted to prePLTs. Two PLTs are generated from a proPLT with the help of the fission event [2]. As a result of the mechanism proceeding at the microscale, employing microfluidic platforms with a high capacity to provide higher shear stress enables the mimicry of the PLT formation from MKs in microchannels. In this way, PLTs can be produced instantaneously from MKs that are isolated and stored in advance.

In recent advances in the development of PLT production, bioreactors aim to mimic the basic physiological properties of bone marrow, including extracellular matrix composition/hardness, tissue-specific microvascular endothelium, blood vessel architecture, and shear stress. However, most of the studies have the characteristic limitations: *i*) failure to achieve targeted PLT production efficiency; *ii*) accumulations, clogging, adhesions within the microchannels; *iii*) inability to predict MK behavior at different shear stresses applied in microchannels [1,3,11-13]. One of the approaches to overcome these constraints is to change design geometries [3,5,11,13-21]. One of the appropriate designs mimics marrow geometry with the concurrent flows as the upper stream has MKs, and the lower one has formed PLTs, separated with microscale slit [1,3,20]. In this geometry, more trapped MKs lead to a higher chance of PLT production. Nakagawa *et al.* [3] proposed that when the upper stream has two inlets, the top flow (pressure flow) pushes the bottom one (MK supply flow) to the slits resulting in a higher amount of MKs trapped within the slits. They experimentally investigated the junction angle between the inlets and concluded that their new bioreactor design, which has 60 degrees between the main and pressure flows, is optimal for increasing the PLT formation yield.

However, this investigation lacks in counting of MKs trapped by the slits due to difficulties of MKs' visualization. Therefore, mathematical modeling is necessary to explore the flow dynamics of trapping of MKs, and investigation of different junction angles and flow rates are required for further design considerations.

This work aims to design and model a microchip platform that will maximize the capture of MKs. The effects of varying flow rates and different structural designs for the microchip on trapping MKs within the slits were studied intensively. In this scope, the effects of flow rate ratios and the junction angle of the inlet channels were investigated by the COMSOL Multiphysics software package. Using tracing mode, we worked on how the MKs interact with the slits to maximize PLT formation. Optimum design and operation conditions were determined with response surface methodology (RSM). A 50.46° angle between the main and the pressure channels, 4.79 for Q_1/Q_2, and 1.13 for Q_3/Q_2 were determined as optimum values. In these optimum conditions, the percentage of trapped MKs was 100, and the relative deviation was <1%.

MODELING AND OPTIMIZATION METHODS

Microfluidic chip design

An illustration of our microfluidic bioreactor is depicted in Figure 1. The height of the channel is taken as 50 μm in our simulations. It has an upper stream, composed of pressure-flow (Q_1) and MK supply flow (Q_2), and a lower stream, called as main flow (Q_3). At the microscale, liquid streams flow laminarly at low Reynolds numbers (Re) - without turbulent mixing [22]. In this way, the flow that includes MKs can be suppressed by the pressure-flow by varying these inlets' flow rates. The widths of the flows (w_1 and w_2) are linearly proportional to their flow

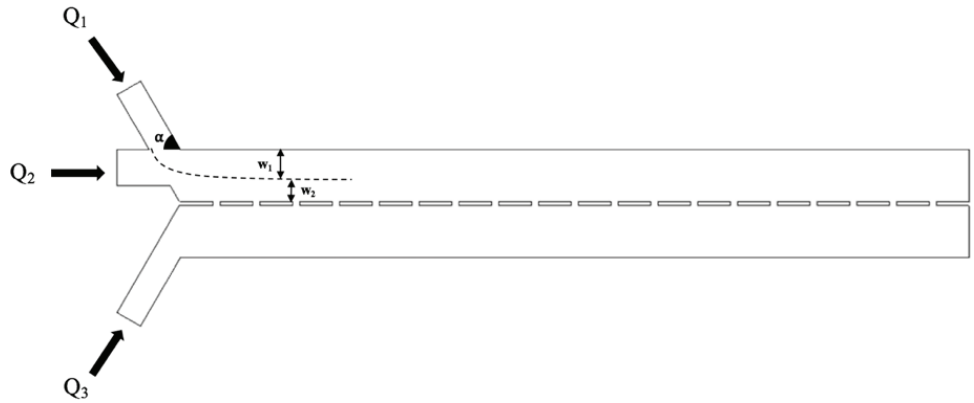

Figure 1. The design of the microfluidic bioreactor.

rates. The inlet configuration of pressure and main streams in our design is *Y*-junction.

We simulated the MKs' behavior in three different configurations. The angles between pressure and main flows are 30, 60, and 90°, respectively. The concurrent flow is separated with the slits with 10 μm wide, 90 μm long, and spaced 20 μm apart. The total flow rate at the upper stream was taken higher than the main flow for the penetration of MKs through the slits. When the MKs are trapped within the slits, the main flow is responsible for the MKs' elongation under the shear stress. The modeling of the MKs' elongation is not within the scope of this work, but we set the flow rate of the main flow based on the appropriate shear rate interval for the MKs' elongation and PLT formation.

COMSOL Multiphysics implementation

Computational fluid dynamics (CFD) is a tool that uses numerical calculations to analyze and solve problems that include fluid flows [23,24]. In our work, computational fluid dynamics was used to simulate and predict the flow regime in the microchannels using COMSOL Multiphysics. We performed two-dimensional space COMSOL simulations to design and model our microchip that will maximize the MKs trapping. We changed the angle between pressure and main flows, and the flow rate ratios of Q_1, Q_2 and Q_3 to determine the velocity profiles and streamlines. Besides, particle tracing mode was used to pursue the particles within the microchannel and optimize PLT trapping. In COMSOL simulation, we chose the boundaries as a wall with no specific material property for the microchip. Water was selected as fluid [25], and solid particles had a 5 μm diameter as an MK.

The governing equations of COMSOL

The equations that represent the single-phase fluid flow interfaces can be obtained by employing of conservation of mass and momentum principles. These equations are given in their most general form in Eqs. (1) and (2):

$$\frac{\partial \rho}{\partial t} + \nabla(\rho \mathbf{u}) = 0 \tag{1}$$

$$\rho \frac{\partial \mathbf{u}}{\partial t} + \rho(\mathbf{u}\nabla)\mathbf{u} = \nabla\left[-p\mathbf{I} + \tau\right] + \mathbf{F} \tag{2}$$

where ρ is the density (SI unit: kg/m^3), $\mathbf{u}$ is the velocity vector (SI unit: m/s), p is pressure (SI unit: Pa), τ is the viscous stress tensor (SI unit: Pa), $\mathbf{I}$ is the unit tensor, $\mathbf{F}$ is the volume force vector (SI unit: N/m^3). Eq. (2) can be reduced to the Navier-Stokes equation for incompressible and Newtonian fluids which is the case for blood.

For a Newtonian fluid, which has a linear relationship between stress and strain, Stokes deduced the following expression (Eq. (3)):

$$\tau = 2\mu\mathbf{S} - \frac{2}{3}\mu(\nabla\mathbf{u})\mathbf{I} \tag{3}$$

$$\mathbf{S} = \frac{(\Delta u) + (\Delta u)^T}{2} \tag{4}$$

The expression for $\mathbf{S}$ is given in Eq. (4) where Δu is the velocity gradient tensor and $(\Delta u)^T$ is the transpose of the velocity gradient tensor.

The particle tracing module is available to assist with modeling problems. It is possible to model particle tracing with COMSOL Multiphysics, provided that the impact of the particles on the flow field is negligible. First, it computes the flow field, and then, as an analysis step, it calculates the motion of the particles. The motion of a particle is defined by Newton's second law (Eq. (5)):

$$\frac{\mathrm{d}^2\mathbf{x}}{\mathrm{d}t^2} = \mathbf{F}(t, \mathbf{x}, \frac{\mathrm{d}\mathbf{x}}{\mathrm{d}t}) \tag{5}$$

where $\mathbf{x}$ is the position of the particle, m the particle mass, and $\mathbf{F}$ is the sum of all forces acting on the particle. Examples of forces acting on a particle in a fluid are the drag force, the buoyancy force, and the gravity force.

The particle Reynolds number is defined as (Eq. (6)):

$$\mathrm{Re}_\mathrm{p} = \frac{\left|\mathbf{u} - \mathbf{u}_\mathrm{p}\right| 2r\rho}{\mu} \tag{6}$$

$\mathbf{u}_\mathrm{p}$ the particle velocity, r the particle radius, ρ the fluid density, and μ the dynamic viscosity of the fluid. The empirical expression for the drag force (Eq. (7)), according to Khan and Richardson is [26]:

$$\mathbf{F} = \pi r^2 \rho \left|\mathbf{u} - \mathbf{u}_\mathrm{p}\right| (\mathbf{u} - \mathbf{u}_\mathrm{p}) \times \\ \times \left[1.84 Re_\mathrm{p}^{-0.31} + 0.239 Re_\mathrm{p}^{0.06}\right]^{3.45} \tag{7}$$

Response surface methodology

RSM is a combination of mathematical and statistical techniques where the response is affected by several variables [27,28]. Therefore, we employed RSM before simulations in order to optimize the MKs trapping by varying geometries and operating conditions. Thanks to RSM, mathematical models (linear, square polynomial functions, and others) gotten with statistical techniques and results obtained with the

help of designed experiments can be verified [29]. A linear function is the simplest model that can be used for the RSM. When the responses are fitted to Eq. (8), the linear model is achieved as:

$$Y = \beta_0 + \sum_{i=1}^{n} \beta_i x_i + \lambda \quad (8)$$

where n is the number of variables, β_0 is the constant term, β_i represents the coefficients of the linear parameters, x_i represents the variables, and λ is an error [30]. The range and levels of independent variables and the numerical values of quantities are displayed in Table 1.

Table 1. Range and levels of independent variables for simulation studies

Independent variable	Range and levels		
	-1	0	+1
Angle (°), X_1	30	60	90
Q_1/Q_2, X_2	2	4	6
Q_3/Q_2, X_3	1	3	5

In the regression equation, the test variables were coded according to Eq. (9):

$$x_{(i)} = \frac{X_i - X_i^*}{\Delta X_i} \quad (9)$$

where $x_{(i)}$ is the coded value of the i-th independent variable, X_i is the uncoded value of the i-th independent variable, X_i^* is the uncoded i-th independent variable at the center point, and ΔX_i is the step change value [28].

In our work, angles between pressure and supply flows and the flow rate ratios of Q_1/Q_2 and Q_3/Q_2 were chosen as the independent input variables, and the response variable was determined as a percentage of trapped particles achieved by COMSOL simulations. The Design Expert software (version 6.01, Stat-Ease, Inc., MN, USA) was used for regression and graphical analysis of the data obtained. The statistical importance of the linear model was determined by the analysis of variance (ANOVA). The effect of each parameter was evaluated by the F-value and the p-value. The characteristic of the fit of the linear model was identified by the R^2 value.

RESULTS AND DISCUSSION

COMSOL modeling

In our design, we mimicked the bone marrow geometry for the trapping of MKs. We first investigated the appropriate range of the flow rates that create a convenient shear rate for MKs elongation by CFD. When the Q_2 was set to 5 μL/min, the flow rate and the shear rate profiles were achieved as in Figure 2A and B, respectively. The flow rate profile and the

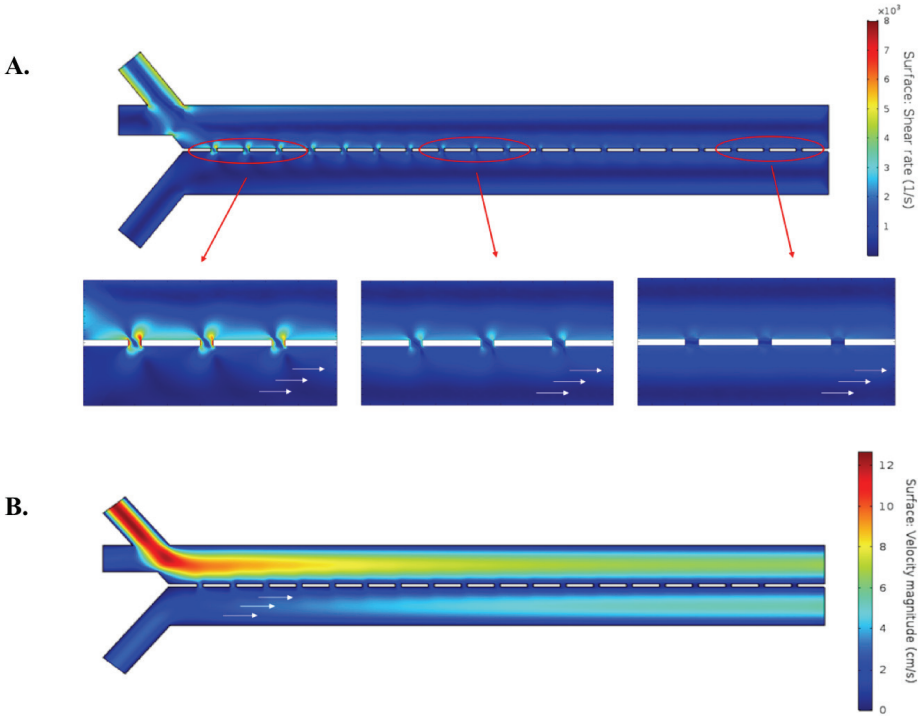

Figure 2. A: Shear rate distribution along the length of the microchip and B: flow rate distribution along the length of the microchip at Q_2 = 5 μL/min (Q_1 = 24 μL/min and Q_3 = 6 μL/min).

shear rate profile are similar throughout the micro-bioreactor.

Contrary to what Thon *et al.* [1] and Martinez *et al.* [20] mentioned, in our design, as it moves along the flow direction into the micro-bioreactor, the shear rate values acting around the slits decrease. The maximum shear rate is 6000 s^{-1} at the first slit, while counting all slits, the average shear rate is 3500 s^{-1}. In the literature, it is possible to find different shear rate values for PLT formation in bioreactors. Even though the shear rate ranges differ from 50 to 6000 s^{-1} in experimental studies, the generally mentioned value range is above 1000 s^{-1} [1,3,13,16,17,19,20]. Therefore, in order to decide the flow rates and predict the shear rates around the slits for the implementation of optimum shear rate ranges for PLT production in our system, we examined flow rates from 1 to 9 µL/min. According to our analyses, the applicable flow rate range is determined as 3 to 8 µL/min by considering shear rate values and as 2 to 5 µL/min by considering maximum shear rate values (Figure 3). The shear rate values required for PLT production in the literature are consistent with the shear rate values we calculated for our design.

Secondly, we examined the effect of the angle between inlet channels (Figure 4A). As shown, 30, 60, and 90° angles were examined at a constant flow rate ratio, respectively. Colorful dots and colorful lines represent the MKs and the streamlines of Q_1, Q_2 and Q_3, respectively. The dots at different velocities are denoted with distinct colors. When the red colored dot moves at the maximum velocity, the blue colored dot is at minimum.

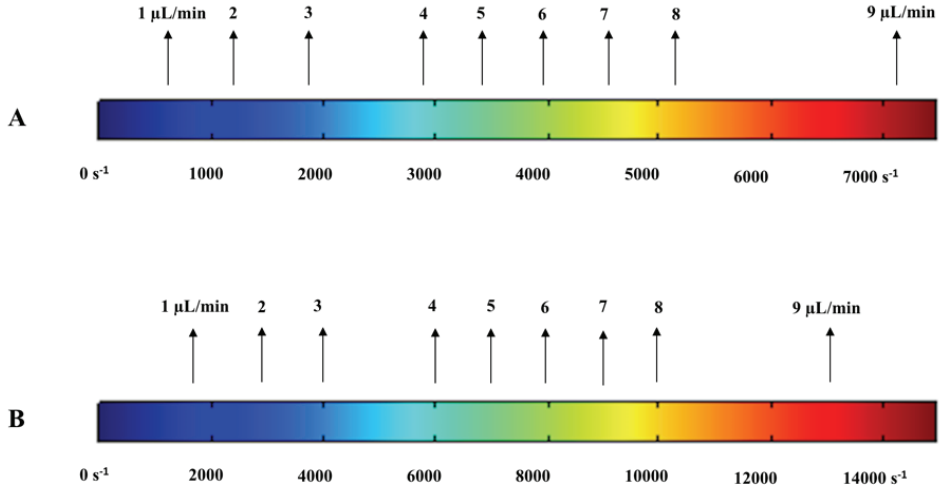

Figure 3. A: Average and B: maximum shear rate ranges at different flow rates.

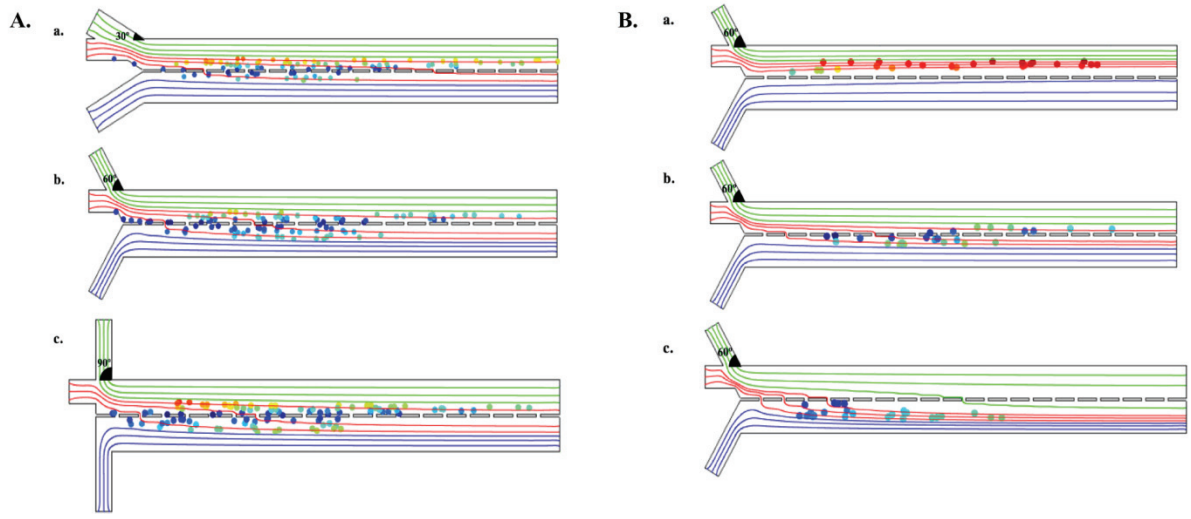

Figure 4. A: Effect of an angle between pressure channels at Q_1 = 10 µL/min, Q_2 = 5 µL/min, Q_3 = 5 µL/min. a: α = 30°, b: α = 60°, c: α = 90°; B: effect of flow rate ratios between main and pressure channels at α = 60°, Q_2 = 5 µL/min. a: Q_1/Q_2 = 2, Q_3/Q_2 = 5, b: Q_1/Q_2 = 4, Q_3/Q_2 = 3, c: Q_1/Q_2 = 6, Q_3/Q_2 = 1.

We can see that more MKs are trapped and pass through the slits when the angle is 60°. The pressure-flow is not very effective when the angle is 30°, resulting in some of the MKs not trapped by the slits. On the other hand, for the design of 90°, the pressure-flow pushes most of the MKs through the first slits. That causes an accumulation of the MKs in that region with losing uniformity of the distribution through the slits. The uniform distribution is critical since once an MK is trapped, the elongation of the MK is not a quick process.

Finally, we explored the effect of flow rate ratios at the 60° angle with different flow rates (Figure 4B). When the Q_3/Q_2 ratio is higher than Q_1/Q_2, the pressures at upper and lower streams are very close to each other. MKs trace the streamlines at the upper stream and cannot pass through the slits. On the contrary, when the Q_1/Q_2 ratio gets higher, and the Q_3/Q_2 is reduced, more MKs diffuse through the slits.

In the literature, only a few studies have a bioreactor design with more than one inlet channel. Thon *et al.* [1] have developed a biomimetic microfluidic PLT bioreactor that recapitulates bone marrow and blood vessel microenvironments, and they reported that their design decreased the PLT release time from 18 to 2 h and increased more than double the PLT yield. The microfluidic bioreactor design has two inlet channels and separated columns spaced 2 μm apart at the center of the bioreactor.

Nakagawa *et al.* [3] designed a new bioreactor with two flows in the concurrent direction, and they reported that designing an angle of 60° between the main and pressure flows promotes PLT generation compared to an angle of 90°. The number of PLTs production increased by 3.6 times with reducing the angle from 90 to 60°. The increase, however, is not explained very well as if it is related to variation in the shear stress or the number of MKs trapped by the slits. Therefore, in this work, we modeled and simulated the flow dynamics in the microfluidic platform.

Response surface methodology

The flow dynamics and particle (MKs) tendency were studied by COMSOL. The effect of the angle and the flow ratios on the MKs trapping were achieved in the previous section. In order to optimize the MKs trapping, optimum operating conditions were determined by RSM. In each run determined by the software, 25 MKs were fed from the MK supply flow. The number of MKs trapped and passed through the slits was counted in order to achieve the yield of each run. The RSM experiments performed and the results obtained under the operational conditions are listed in Table 2. The linear model equation is given below for the actual value (Eq. (10)):

$$Y = 30.96 + 0.25X_1 + 16X_2 - 17.75X_3 \quad (10)$$

where Y is the percent of trapped MKs.

Table 2. The actual values of the simulation conditions and response variables

#	Angle (°)	Q_1/Q_2	Q_3/Q_2	Trapped MK (%)
1	60	4	3	72
2	30	6	3	56
3	90	2	3	8
4	60	4	3	68
5	90	6	3	100
6	60	2	5	0
7	60	4	3	72
8	60	4	3	72
9	30	4	5	0
10	60	4	3	72
11	90	4	1	100
12	30	4	1	100
13	30	2	3	0
14	60	2	1	64
15	60	6	5	72
16	90	4	5	8
17	60	6	1	100

In Table 3, the model *F*-value of 17.97 implies the model is significant. There is only a 0.01% chance that a "Model *F*-Value" this large could occur due to noise. Values of *Prob* > *F* less than 0.05 indicate model terms are significant. In this case, X_2 (0.0003) and X_3 (0.0001) are significant model terms. For the model, *Prob* > *F* (<0.0001) less than 0.05 indicates that the model represents the system well. Adeq Precision measures the signal-to-noise ratio. A ratio greater than 4 is desirable. For the model, the ratio of 14.93 indicates an adequate signal. This model can be used to navigate the design space.

These results show that the effects of Q_1/Q_2 and Q_3/Q_2 directly affect the percentage of trapped MKs. The response surface contour-plots (Figure 5A-C) were drawn to predict the effects of the independent variables on the percentage of trapped MKs. Each contour curve represents an infinite number of combinations of two test variables, with the other two maintained at their respective zero levels.

The percentage of trapped MKs increases with an expansion of angle between pressure flow and main flow (Figure 5A and C). In fact, the increase of trapped MKs percentage is not continuous with the increment in the angle in the preliminary simulations

(Figure 4A). After a specific value, the increase in the angle decreases efficiency. According to the RSM results, the percentage of trapped MKs increases as the angle increases. In addition to the angle increase, the change of Q_1/Q_2 ratio is much higher than the Q_3/Q_2 ratio is more effective.

Table 3. ANOVA for response surface linear model

Source	Sum of squares	*df*	Mean square	*F*-Value	*p*-Value *Prob* > *F*
Model	18724	3	6241.33	17.97	< 0.0001
X_1	450	1	450	1.30	0.2756
X_2	8192	1	8192	23.58	0.0003
X_3	10082	1	10082	29.03	0.0001
Residual	4515.53	13	347.35		
Lack of fit	4502.73	9	500.30	156.34	< 0.0001
Pure error	12.8	4	3.2		
Cor. total	23239.53	16			
R^2 = 0.81					
Adeq. precision = 14.93					

The percentage of trapped MKs increases with increasing the ratio of Q_1/Q_2 (Figures 5A-5B). In our design, Q_1 has an impact on Q_2 in which Q_2 is pressed from above, and more MKs come to contact with the slits. This case is explained by the laminar flow behavior in microchannels. The widths of the Q_1 and Q_2 flows are precisely equal to the flow rate ratio of these flows. When the value of Q_1 becomes higher than Q_2, the width of Q_2 flow shrinks and MKs in this flow comes closer to the slits.

The flow of Q_3 is responsible for the elongation of the MKs to produce the PLTs. Although we did not study the MKs' elongation dynamics, we take account of the shear rate interval corresponding to PLT generation. The interval of the shear rate is taken as *X*-*Y* unit in this study. Moreover, the optimization of our design excludes the number of PLT formation, so optimization only deals with it if the Q_3 has a capacity for generating an appropriate shear rate. The percentage of trapped MKs decreases with an increasing Q_3/Q_2 ratio (Figure 5B and C). An increase in this ratio

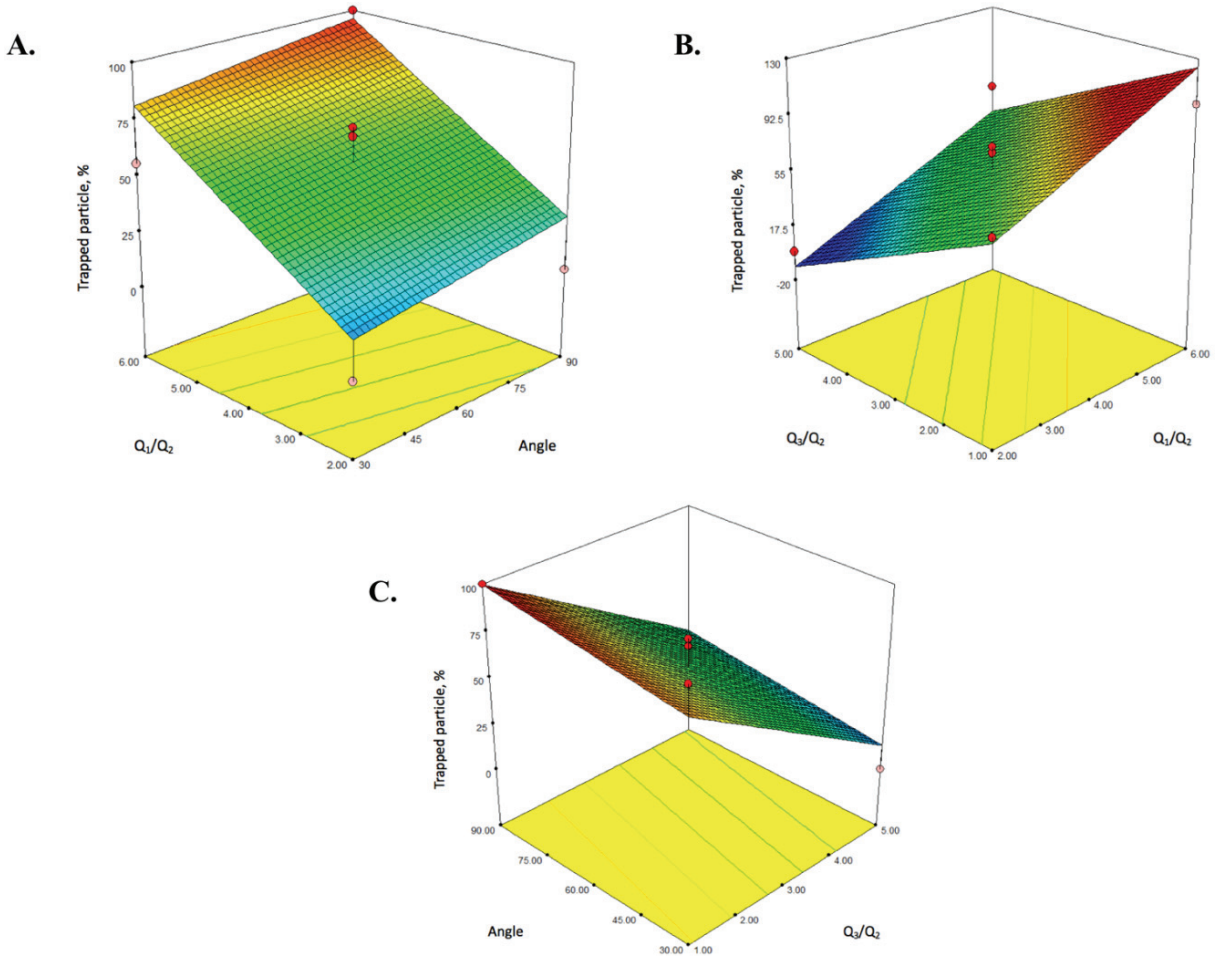

Figure 5. A: Contour-plot of the percentage of trapped particles: the effect of Q_1/Q_2 and angle. Q_1 = 5 μL/min; B: contour-plot of the percentage of trapped particles: The effect of Q_3/Q_2 and Q_1/Q_2. Q_1 = 5 μL/min; C: contour-plot of the percentage of trapped particles: the effect of angle and Q_3/Q_2. Q_1 = 5 μL/min. The other variable is held at zero level.

promotes a negative pressure effect that pushes upwards of MKs and prevents penetration through the slits. In other words, MKs are directed to the upper stream.

To maximize the percent of trapped MKs, we obtained the optimum conditions given in Table 4 by RSM. With these optimum values, the percentage of trapped MKs was obtained as 100%. In order to verify these results, a simulation study was carried out at these conditions, and the percentage of trapped MKs was achieved as 100. The relative deviation between the RSM analysis and the COMSOL simulations was computed as <1%. In Figure 6, MKs' locations can be seen clearly at different times in a microchannel at the optimum values of angle, Q_1, Q_2 and Q_3 in COMSOL simulation. At the end of the process, the entirety of MKs pass through the slits.

Table 4. Optimum values of independent variables obtained with RSM

Independent variable	Optimum value
Angle (°)	50.46
Q_1/Q_2	4.79
Q_3/Q_2	1.13

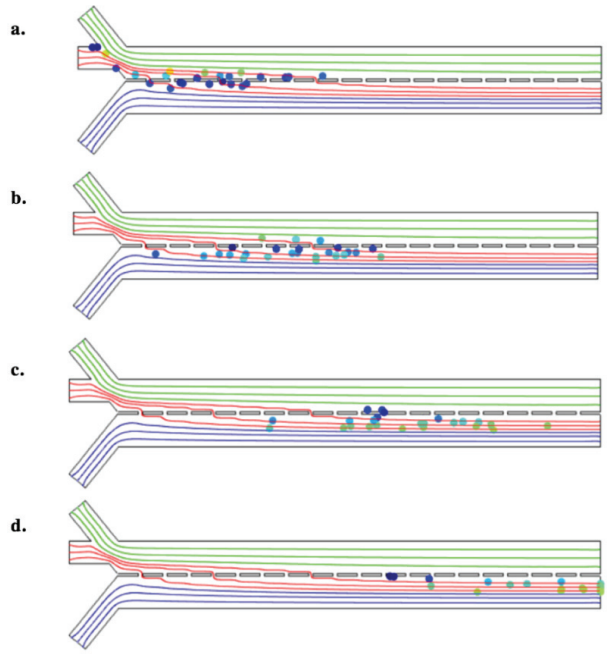

Figure 6. MKs' locations at different times in a microchannel at the optimum values of physical conditions. α = 50.46°, Q_1 = 23.95 μL/min, Q_2 = 5 μL/min, Q_3 = 5.65 μL/min. a: Near the beginning time of the process; b: near the mid-time of the process; c: after the mid-time of the process; d: near the end time of the process.

After exploring the literature, this study is probably the first one that includes tracing of MKs and observing their attitude under different conditions and designs PLT generation. It is known that computational fluid dynamics modeling is necessary for the fluid dynamics on MKs to be well-understood [14]. We believe that with the help of simulation and modeling studies, the PLT production yield can be increased in a short time because once the well-understood flow behaviors of MKs are provided, less effort will be made on performing experimental studies. Our future direction is modeling MKs' elongation to produce PLT and merging it with our current study. In this way, it will extend our knowledge for fabricating highly efficient bioreactors for PLT generation.

CONCLUSION

The bioreactors which we recommend for use in the production of PLTs from MKs should be designed to maximize the amount and rate of platelet production. Optimally designed microchannels, acting as bioreactors, increase the surface area of MKs to allow platelet formation, mimic shear stress in blood flow, and trigger PLT release. Here, the most effective control parameter for optimal design is the shear stress, as well as the flow rate, and the shear stress to maximize the amount and rate of PLT production within the microchannel can only be adjusted by the angle of entry. The flow rate, which is defined as the ratio of the pressure flow to the main flow, is directly proportional to the velocity of the fluid in the microchannel; the higher the speed the more velocity gradient, the higher the shear stress for a certain inlet angle.

The process of PLT production from MKs can be analyzed as having two stages; the first one is trapping the MKs, and the second one is the elongation of proPLTs. In this study, we only focused on the first step of the process, aiming to trap more MKs with the assistance of the flow pressure. It is an undeniable fact that the angle between the main and pressure flows should be close to 60°, as indicated in the literature [1]. While current studies give the results over PLT production efficiency, the results are given on the trapping of MKs in this study. Although the approach is different, our simulation results overlap with the literature data. These results indicate that our approach is promising. Based on our simulation and optimization results, the ultimate MKs trapping is achieved when the angle is 50.46°. On the other hand, we conclude that the contribution of the ratio of pressure flow to the main flow is more significant than the angle between the flow directions on the percent-

age of trapped MKs. If the nature of PLT formation is considered, the effect of the angle between the main and pressure flows alone will not be sufficiently effective unless the required trapping and elongation effects occur. In this study, since the microchannels' width is large enough, 2D modeling has been made to simplify the system. Also, 2D modeling was preferred instead of 3D because, in 2D modeling, much higher spatial and temporal resolution can be obtained numerically compared to a comparable three-dimensional simulation [31]. Besides, 2D can be used instead of 3D in cases where the channel width effect is neglected [32,33].

It is clear that biological particles' physical interaction with the microchannel walls is meaningful [34]. However, we ignored that this interaction may be a limitation in our simulations. From a general perspective, it is necessary to examine the passage of MKs through slits more regularly. The best results will be achieved by taking into account the elongation process after passing through slits.

Nomenclature

PLT	Platelet
MK	Megakaryocyte
Q_1	Flow rate of pressure flow
Q_2	Flow rate of megakaryocyte supply flow
Q_3	Flow rate of main flow
α	Angle between main and pressure channels
w_1	Width of pressure flow in microchannel
w_2	Width of megakaryocyte supply flow in microchannel
Re	Reynolds number
CFD	Computational fluid dynamics
RSM	Response surface methodology

Acknowledgement

The authors wish to express appreciation to Dr. Huseyin Uvet from the Yildiz Technical University Department of Mechatronics Engineering (Istanbul, Turkey) for critical advising and enabling the use of COMSOL Multiphysics (Version 5.3 CPU License No: 17076072).

Funding

This work was supported by Research Fund of the Yildiz Technical University. Project number FCD--2018-3150.

REFERENCES

[1] J.N. Thon, L. Mazutis, S. Wu, J.L. Sylman, A. Ehrlicher, K.R. Machlus, Q. Feng, S. Lu, R. Lanza, K.B. Neeves, D.A. Weitz, J.E. Italiano Jr., Blood 124 (2014) 1857–1867

[2] K.R. Machlus, J.E. Italiano, J. Cell Biol. 201 (2013) 785–796

[3] Y. Nakagawa, S. Nakamura, M. Nakajima, H. Endo, T. Dohda, N. Takayama, H. Nakauchi, F. Arai, T. Fukuda, K. Eto, Exp. Hematol. 41 (2013) 742–748

[4] T. Matsunaga, I. Tanaka, M. Kobune, Y. Kawano, M. Tanaka, K. Kuribayashi, S. Iyama, T. Sato, Y. Sato, R. Takimoto, T. Takayama, J. Kato, T. Ninomiya, H. Hamada, Y. Niitsu, Stem Cells 24 (2006) 2877–2887

[5] A.C. Schlinker, K. Radwanski, C. Wegener, K. Min, W.M. Miller, Biotechnol. Bioeng. 112 (2015) 788–800

[6] Y. Ito, S. Nakamura, N. Sugimoto, T. Shigemori, Y. Kato, M. Ohno, S. Sakuma, K. Ito, H. Kumon, H. Hirose, H. Okamoto, M. Nogawa, M. Iwasaki, S. Kihara, K. Fujio, T. Matsumoto, N. Higashi, K. Hashimoto, A. Sawaguchi, K. Harimoto, M. Nakagawa, T. Yamamoto, M. Handa, N. Watanabe, E. Nishi, F. Arai, S. Nishimura, K. Eto, Cell 174 (2018) 636-648

[7] T.J. Cobain, E.C. Vamvakas, A. Wells, K. Titlestad, Transfus. Med. 17 (2007) 1–15

[8] M.T. Sullivan, R. Cotten, E.J. Read, E.L. Wallace, Transfusion 47 (2007) 385–394

[9] G. Ingavle, N. Shabrani, A. Vaidya, V. Kale, Acta Biomater. 96 (2019) 99–110

[10] J.N. Thon, J.E. Italiano, Semin. Hematol. 47 (2010) 220–-226

[11] I. Pallotta, M. Lovett, D.L. Kaplan, A. Balduini, Tissue Eng., C 17 (2011) 1223–1232

[12] Q. Feng, N. Shabrani, J.N. Thon, H. Huo, A. Thiel, K.R. Machlus, K. Kim, J. Brooks, F. Li, C. Luo, E.A. Kimbrel, J. Wang, K. Kim, J. Italiano, J. Cho, S. Lu, R. Lanza, Stem Cell Reports 3 (2014) 817-831

[13] C.A. Di Buduo, L.S. Wray, L. Tozzi, A. Malara, Y. Chen, C.E. Ghezzi, D. Smoot, C. Sfara, A. Antonelli, E. Spedden, G. Bruni, C. Staii, L. De Marco, M. Magnani, D. L. Kaplan, A. Balduini, Blood 125 (2015) 2254-2264

[14] J.N. Thon, B.J. Dykstra, L.M. Beaulieu, Platelets 28 (2017) 472–477

[15] B. Sullenbarger, J. Hwan Bahng, R. Gruner, N. Kotov, L.C. Lasky, Exp. Hematol. 37 (2009) 101–110

[16] C. Dunois-Lardé, C. Capron, S. Fichelson, T. Bauer, E. Cramer-Bordé, D. Baruch, Blood 114 (2009) 1875–1883

[17] A. Blin, A. Le Goff, A. Magniez, S. Poirault-Chassac, B. Teste, G. Sicot, K.A. Nguyen, F.S. Hamdi, M. Reyssat, D. Baruch, Sci. Rep. 6 (2016) 1–8

[18] W.B. Mitchell, M.P. Avanzi, New York Blood Center, Inc, assignes. United States Patent US 9,574,178. Feb 21 (2017)

[19] M.P. Avanzi, W.B. Mitchell, Br. J. Haematol. 165 (2014) 237-247

[20] A.F. Martinez, R.D. McMahon, M. Horner, W.M. Miller, Biotechnol. Prog. 33 (2017) 1614–1629

[21] S.M. Hastings, M.T. Griffin, D.N. Ku, Platelets 28 (2017) 427–433

[22] P.J.A. Kenis, R.F. Ismagilov, G.M. Whitesides, Science 285 (1999) 83-85

[23] S.M. Rahman, V. Hlady, Lab Chip 21 (2021) 174-183

[24] O. Ulkir, O. Girit, I. Ertugrul, J. Nanometer. 2021 (2021) 1-10

[25] I. Ertugrul, O. Ulkir, RSC Adv. 10 (2020) 33731-33728

[26] Multiphysics C.: CFD Module User 's Guide. COMSOL Multiphysics (2016)

[27] G. Baydar Atak, E. Bayraktar, U. Mehmetoglu, Green Process. Synth. 8 (2019) 525-532

[28] E. Bayraktar, Process Biochem. 37 (2001) 169-175

[29] G. Ye, L. Ma, L. Li, J. Liu, S. Yuan, G. Huang, Int. J. Coal Prep. Util. 40 (2017) 1-15

[30] M.A. Bezerra, R.E. Santelli, E.P. Oliveira, L.S. Villar, L.A. Escaleira, Talanta 76 (2008) 965-977

[31] G. Boffetta, R.E. Ecke, Annu. Rev. Fluid Mech. 44 (2012) 427-451

[32] Y. Zhang, X. Chen, J. Braz. Soc. 89 (2020) 1-11

[33] Y. Zhang, X. Chen, J. Braz. Soc. 206 (2020) 1-11

[34] Z.B. Sendekia, P. Bacchin, Langmuir 32 (2016) 1478--1488.

GUNAY BAYDAR-ATAK[1]
MERT AKIN INSEL[1]
MUHAMMED ENES ORUC[2]
HASAN SADIKOGLU[1]

[1]Yildiz Technical University, Department of Chemical Engineering, Esenler, İstanbul, Turkey
[2]Gebze Technical University, Department of Chemical Engineering, Gebze, Kocaeli, Turkey

NAUČNI RAD

OPTIMIZACIJA ZAROBLJAVANJA MEGAKARIOCITA ZA FORMIRANJE TROMBOCITA U MIKROKANALIMA

Trombociti su odgovorni za zaustavljanje krvarenja. Oni su mali fragmenti ćelija proizvedeni od megakariocita u koštanoj srži. Mali broj trombocita je značajan zdravstveni problem za pacijenta. Trombociti mogu da se čuvaju obično do 5 dana pre transfuzije. Trenutna proizvodnja trombocita iz izolovanih i uskladištenih megakariocita je ključna za zdravlje pacijenta. Zahvaljujući mikrofluidnim platformama, trombociti se mogu trenutno proizvesti iz megakariocita. Ovde je računarski proučavana dinamika fluida u mikrokanalima sa strukturama proreza i različitim geometrijama ulaza. Analiza dinamike strujanja je izvršena pomoću komercijalnog softvera. Istraživani su uticaji protoka i ugla između ulaznih kanala na zarobljavanje megakariocita. Optimizacija ugla između ulaznih kanala i protoka glavnog i potisnog toka je urađena metodologijom površine odziva brojanjem zarobljenih megakariocita. Pri optimalnim uslovima procenat zarobljenih megakariocita je bio 100 sa relativnim odstupanjem manjim od 1%. Takođe, zaključeno je da je za hvatanje veće količine megakariocita protok jednako važan kao i ugao između ulaznih kanala.

Ključne reči: mikrofluidika, biotehnologija, matematičko modeliranje, trombociti, COMSOL.